

High Resolution Distributed Strain or Temperature Measurements in Single- and Multi-mode Fiber Using Swept-Wavelength Interferometry

Stephen T. Kreger, Dawn K. Gifford, Mark E. Froggatt, Brian J. Soller, Matthew S. Wolfe

Luna Technologies, 3157 State Street, Blacksburg, VA 24060.

kregers@lunatechnologies.com

Abstract: We describe the use of swept-wavelength interferometry for distributed fiber-optic strain and temperature sensing in single mode and gradient index multimode fiber. The method is used to measure strain in a four-strand multimode cable under twist.

1. Introduction

Methods currently available for distributed strain or temperature sensing in optical fiber include techniques based on Raman, Brillouin, and Rayleigh scattering as well as those involving dense multiplexing of fiber Bragg gratings (FBGs) [1-4]. Techniques based on scatter typically employ optical time domain reflectometry and are thus limited in spatial resolution to 0.1 to 1 m. FBG methods are often limited by the number of gratings that can be multiplexed in a single fiber, and gratings in multimode fiber are wideband or multiple-peaked, limiting their usefulness [5].

We present a technique for measuring distributed strain or temperature with high spatial resolution using standard telecom-grade single mode and gradient index multimode fibers. We use swept wavelength interferometry (SWI) to measure the Rayleigh backscatter as a function of length in optical fiber with high spatial resolution [6]. A sensor element is formed by transforming a spatial segment of the Rayleigh backscatter pattern into the optical frequency domain and measuring the induced shift in the reflected spectrum. While a similar method has previously been used to measure distributed strain [7], recent advancements in measurement instrumentation represent at least an order of magnitude improvement in spatial and spectral resolution. Furthermore, we demonstrate that there is no significant loss of spectral or spatial resolution over our instrument's range of 30 m when using gradient index multimode as the sensing fiber. Finally, we apply the technique to measure strain in a four-strand multimode cable.

2. Measurement Method

Rayleigh backscatter in optical fiber is caused by random fluctuations in the index profile along the fiber length. For a given fiber, the scatter amplitude as a function of distance is a random but static property of that fiber and can be modeled as a long, weak FBG with a random period. Changes in the local period of the Rayleigh scatter caused by an external stimulus (like strain or temperature) in turn cause shifts in the locally reflected spectrum. These local spectral shifts can then be calibrated and assembled to form a distributed strain or temperature measurement.

The instrument uses polarization-diverse SWI to measure both the amplitude and phase of the Rayleigh backscatter signal [8]. The measurement network used is shown in Figure 1. Light from an external-cavity tunable laser source (TLS) is split between the reference and measurement arms of an interferometer. In the measurement path, a 50/50 coupler further splits the light to interrogate a length of fiber under test (FUT) and returns the reflected light. Another 50/50 coupler then recombines the measurement and reference fields. A polarization beam splitter and a polarization controller are used to split the reference light evenly between two orthogonal polarization states. As the laser is linearly tuned in frequency the interference between the measurement field and these two polarization states is then recorded at detectors labeled S and P. The Rayleigh scatter as a function of length is obtained via a Fourier transform (see reference [6] for details).

When multimode fiber is used as the FUT, a SMF-28e lead is spliced to the multimode fiber by matching up cladding edges; no special mode launch conditions are attempted. This launch condition heavily favors the central modes of the multimode fiber. Although modal dispersion causes the Rayleigh backscatter to blur over distance, at the 30 m range limit of our instrument the modal dispersion length is less than 1 mm.

A distributed sensor is formed by first measuring and storing the Rayleigh scatter signature of the FUT at an ambient temperature and null strain state. Then the scatter profile is measured at a later time with strain or a temperature perturbation applied to the fiber. The complex data sets from each detector, S and P, are broken into interval lengths Δz along the FUT are Fourier transformed into the optical frequency domain. A vector sum of

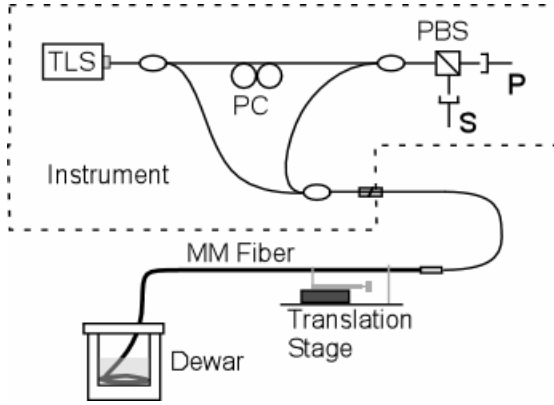


Fig. 1. Optical network used for polarization-diverse measurement of Rayleigh backscatter.

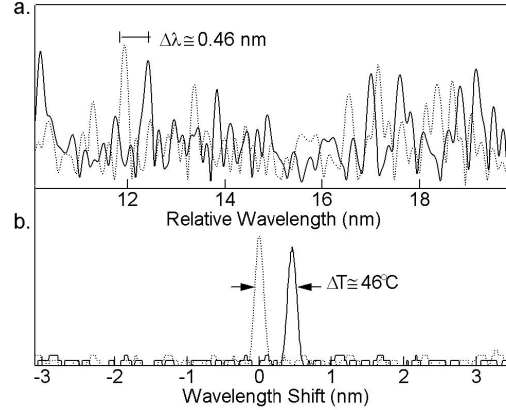


Fig. 2. a. Wavelength spectra along a 5 mm fiber interval for a heated (solid) and unheated (dotted) measurement scan. b. Cross-correlation of the heated spectra with reference (unheated) spectrum.

the S and P spectra is then calculated to generate a polarization-independent spectrum associated with each interval. To determine the spectral shift between the reference and perturbed scans, a cross-correlation is performed for each FUT interval. Any change in strain or temperature manifests as a shift in the correlation peak. A distributed measurement is formed by compiling the spectral shifts for each interval along the FUT.

Figure 2a shows the fiber Rayleigh backscatter spectra along a 5mm segment for a reference scan at ambient temperature and scan of the same fiber interval after heating. Fig. 2b then shows the cross-correlation with the reference spectrum for a measurement scan with and without temperature shift. The spectral difference between the shifted peak and the un-shifted peak is directly proportional to the temperature shift in this fiber interval.

It is important to note that the interval length Δz affects the signal-to-noise ratio of the shift - a wider Δz incorporates more data points and gives better spectral resolution. However, if the local spectral shift varies significantly over Δz the cross correlation peak may spread out and become difficult to detect, resulting in higher noise levels. Thus in fiber sections where there is a strong temperature or strain gradient reducing Δz often produces a more stable result.

3. Strain and Temperature Calibration

The spectral “fingerprint” of the Rayleigh backscatter may be thought of as a weak Bragg grating with randomly varying period. In the case of a standard Bragg grating, the resonant wavelength of a Bragg grating reflection is determined by the effective line spacing and effective index of refraction, n . Changes in these parameters shift the grating’s resonant wavelength. The spectrum of the Rayleigh backscatter pattern responds in the same manner: changes in refractive index or physical length shift the reflected spectrum in frequency. The physical length and index of refraction of the fiber are intrinsically sensitive to environmental parameters temperature and strain and, to a much lesser extent, pressure, humidity (if the fiber coating is hygroscopic), electromagnetic fields, etc [9-11]. The wavelength shift, $\Delta\lambda$, or frequency shift, $\Delta\nu$, of the backscatter pattern due to a temperature change, ΔT , or strain along the fiber axis, ϵ , is identical to the response of a fiber Bragg grating:

$$\Delta\lambda/\lambda = -\Delta\nu/\nu = K_T\Delta T + K_\epsilon\epsilon \quad (1)$$

The temperature coefficient K_T is a sum of the thermal expansion coefficient and the thermo-optic coefficient, with typical values of $0.55 \times 10^{-6} \text{ }^\circ\text{C}^{-1}$ and $6.1 \times 10^{-6} \text{ }^\circ\text{C}^{-1}$ for Germania-doped silica core fibers. The strain coefficient is a function of n ; the components of the strain-optic tensor, p_{ij} ; and Poisson’s ratio, μ . Typical values given for n , p_{12} , p_{11} and μ for germanium-doped silica yield a value for K_ϵ of 0.787. Thus a shift in temperature or strain is merely a linear scaling (for moderate temperature and strain ranges) of the spectral frequency shift $\Delta\nu$.

The strain and temperature coefficients of a particular fiber type may be calibrated in a straightforward manner by recording the spectral shift for a known applied strain or temperature shift. In all measurements below the laser source was tuned over 40 nm with a center wavelength of 1550 nm. The data acquisition rate limited range to a length of 30 m with a 0.020 mm ultimate spatial resolution. Each measurement took less than 5 s for the 40 nm wavelength scan and associated calculations. Measurements were performed on 5 m long segments of Corning SMF-28e single mode fiber and Corning InfiniCor 300 gradient index multimode fiber.

Strain was precisely induced in the fiber by mounting a stainless steel linear bearing translation stage with a 1 micron resolution micrometer drive on an aluminum rail and clamping the fiber on the stage and on a distant point

on the rail. In this manner tensile strains over the range of 0 to 5000 $\mu\epsilon$ with a total gage length of 320 mm were generated. Fusion splice protector tubes were used to grip the fiber; the splice protectors were clamped down to the linear stage and rail. A typical spectral shift as a function of fiber position for the strained section of the FUT is shown in Figure 3. The gradual roll-off of the spectral shift profile indicated that the strain gradually decreased to zero at 35 mm into the 40 mm long splice protector.

The same section of fiber was removed from the strain apparatus and coiled at the bottom of a covered glass dewar. Hot water was introduced and increasingly diluted with chilled water, producing bath temperatures in the range of 80 to 5 C. The temperature was measured using a type K thermocouple. Temperature and spectral shift readings were taken several minutes after each dilution to allow the apparatus to reach thermal equilibrium. A typical plot of the spectral shift as a function of fiber position for a section of the FUT from outside of the dewar to the coil at the bottom of the dewar is shown in Figure 4. The fiber entered the top of the dewar at position $z = 2.32$ m and dropped below the water level at $z = 2.66$ m. The effects of strain build up at the edge of the splice protectors and the higher thermal expansion coefficient of the steel rod in the splice protector are observed at positions 3.07 m and 3.40 m.

Values measured for the strain coefficient and temperature coefficient for the two fiber types are displayed in Table 1. Compared to coefficient values listed in references [9-11], the values are roughly 5% lower for K_ϵ and 10% higher for K_T . The differences are likely indicative of slight dopant level and coating material differences. The standard deviations of the fit residuals, listed in Table 1, are an indication of the uncertainty of an individual measurement over the calibration range. The listed values compare favorably to the estimated strain uncertainty stemming from the resolution of the micrometer, 3.1 $\mu\epsilon$, and the estimated temperature uncertainty of the thermocouple, 0.5 $^\circ\text{C}$.

The best-case noise-limited resolution can be estimated by computing the standard deviation of a series of spectral shift measurements when temperature and strain are held constant between scans. Figure 5 shows the estimated resolution for various settings of the interval size Δz . At most Δz values the multimode sample has a slightly higher noise level because of an additional 0.9 dB insertion loss at the single mode to multimode splice. Below a segment size of 5 mm, noise levels increase as the number of data points included in the Fourier Transform and cross correlation calculations are diminished. Above 5 mm, the noise floor stabilizes and starts to increase as

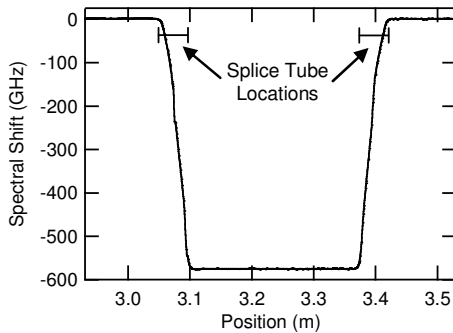


Fig. 3. Spectral shift as a function of fiber position for the case of 4000 $\mu\epsilon$ applied strain using a 5 mm interval size.

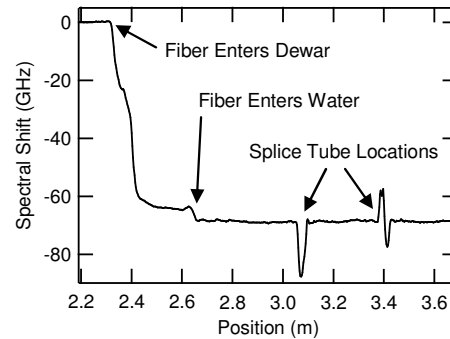


Fig. 4. Spectral shift as a function of fiber position for the case of coiled fiber immersed in a water bath at 76.6 $^\circ\text{C}$ using a 10 mm interval size.

Table 1. Strain and Temperature coefficients and fit residual standard deviations for two fiber types.

Fiber Type	K_ϵ	σ_ϵ resid	K_T	σ_T resid
SMF-28e	0.7314 ± 0.0006	3.0 $\mu\epsilon$	7.09 ± 0.04 $\times 10^{-6} \text{ } ^\circ\text{C}^{-1}$	0.4 $^\circ\text{C}$
InfiniCor 300	0.7484 ± 0.0004	1.3 $\mu\epsilon$	7.64 ± 0.04 $\times 10^{-6} \text{ } ^\circ\text{C}^{-1}$	0.4 $^\circ\text{C}$

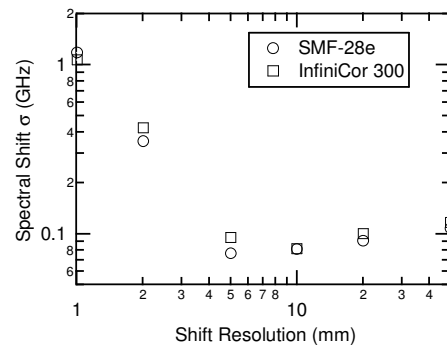


Fig. 5. Spectral resolution as a function of interval size, Δz . Noise increases rapidly as Δz is reduced below 5 mm.

real shifts in temperature and strain along the segment dominate the calculation. Given 0.1 GHz as the best-case spectral shift resolution, the resulting strain and temperature resolutions are $0.8 \mu\epsilon$ and $0.08 \text{ }^\circ\text{C}$, respectively.

4. Distributed Strain in Multimode Fiber Example

An example of a distributed strain measurement that benefits from the high spatial resolution of our instrument is the strain profile of a multimode fiber in a four-fiber heavy duty cable under twist, as shown in Figure 6. The induced twist resulted in a highly variable level of tensile strain on the fiber. The average and maximum strains monitored on the 4 m length of cable are depicted in Figure 7. Using the fiber manufacturer's guideline for the maximum safe tensile stress of 20 kpsi to ensure a 40 yr installation lifetime [12], the suggested maximum twist rate for this cable is 3.3 full turns per m. Monitoring fiber strain in this direct manner to determine safe installation limit is highly preferable to relying on strain estimates derived from mechanical modeling.

5. Conclusions

Our SWI technique is highly capable of measuring the spectral shift in the Rayleigh backscatter along an optical fiber with high spatial resolution and spectral sensitivity. The linear relationship between strain or temperature and the spectral shift enables distributed sensing along any standard single-mode or gradient index multimode fiber with millimeter-range spatial resolution over tens of meters of fiber with strain and temperature resolution better than $1 \mu\epsilon$ and $0.1 \text{ }^\circ\text{C}$. The instrument is robust and simple to use. In addition, as the measurement does not require specialty fiber or discrete elements, sensors are very economical.

6. References

- [1] A. J. Rogers, "Distributed optical-fiber sensing," *Meas. Sci. Technol.* **10**, 75-99 (1999).
- [2] M. A. Davis, A. D. Kersey, "Simultaneous measurement of temperature and strain using fiber Bragg gratings and Brillouin scattering," *Proc. SPIE*, **2838**, 114-123 (1996).
- [3] A. J. Rogers, S. V. Shatalin, S. E. Kanellopoulos, "Distributed measurement using optical fibre backscatter polarimetry," *Proc. SPIE*, **5502**, 463-467 (2004).
- [4] M. Froggatt, B. Soller, D. Gifford, and M. Wolfe, "Correlation and keying of Rayleigh scatter for loss and temperature sensing in parallel optical networks," *OFC Technical Digest*, paper PDP 17 (Los Angeles, March 2004).
- [5] T. Mizunami, T. V. Djambova, T. Niiho, and S. Gupta, "Bragg gratings in multimode and few-mode optical fibers", *J. Lightwave Technol.*, **18**, 230-234, (2000).
- [6] B. J. Soller, M. Wolfe, M. E. Froggatt, "Polarization resolved measurement of Rayleigh backscatter in fiber-optic components," *OFC Technical Digest*, Los Angeles, March, 2005, paper NWD3.
- [7] M. Froggatt and J. Moore, "High resolution strain measurement in optical fiber with Rayleigh scatter," *Appl. Opt.*, **37**, 1735-1740 (1998).
- [8] B. J. Soller, D. Gifford, M. Wolfe, and M. Froggatt, "High resolution optical frequency domain reflectometry for characterization of components and assemblies," *Opt. Express*, **13**, 666-674 (2005).
- [9] K. O. Hill, G. Meltz, "Fiber Bragg grating technology - fundamentals and overview," *J. Lightwave Technol.*, **15**, 1263-1274 (1997).
- [10] A. D. Kersey, M. A. Davis, H. J. Patrick, M. LeBlanc, and K. P. Koo, "Fiber grating sensors," *J. Lightwave Technol.*, **15**, 1442-1462 (1997).
- [11] A. Othonos, "Fiber Bragg gratings," *Rev. Sci. Instrum.*, **68**, 4309-4340 (1997).
- [12] R. J. Castilone, "Mechanical Reliability: Applied Stress Design Guidelines," Corning White Paper WP5053 (2001).

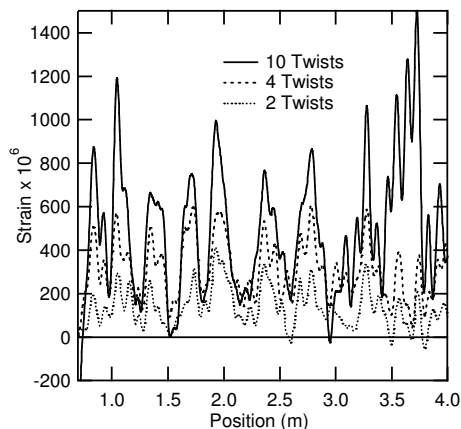


Fig. 6. Distributed strain in a multimode fiber in a four-strand cable as a function of twist number.

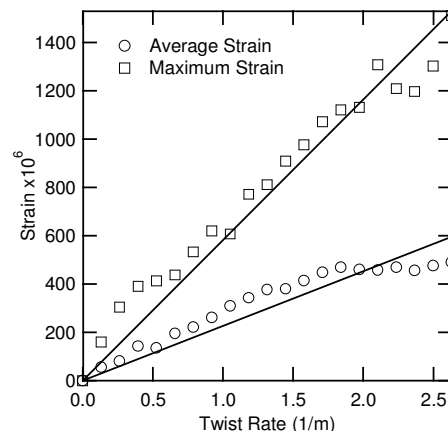


Fig. 7. Average and maximum strain in a multimode fiber in a four-strand cable as a function of twist rate.